UPGRADE OF THE LHC BEAM DUMPING PROTECTION ELEMENTS

W. Weterings, T. Antonakakis, B. Balhan, J. Borburgh, B. Goddard, C. Maglioni, R. Versaci
CERN, Geneva, Switzerland

Abstract

The Beam Dumping System for the Large Hadron Collider comprises for each ring a set of horizontally deflecting extraction kicker magnets, vertically deflecting steel septa, dilution kickers and finally, a couple of hundred meters further downstream, an absorber block. A mobile diluter (TCDQ) protects the superconducting quadrupole immediately downstream of the extraction as well as the arc at injection energy and the triplet aperture at top energy from bunches with small impact parameters, in case of a beam dump that is not synchronized with the particle free gap or a spontaneous firing of the extraction kickers. Simulations have shown that an asynchronous dump of a 7 TeV nominal beam into the TCDQ absorber blocks could damage it. This paper describes the proposed changes to this device in order to maintain the protection for the downstream elements while reducing the risk of damaging the TCDQ in case of such a beam loss.

INTRODUCTION

The LHC beam dumping system (LBDS) is composed of an extraction kicker magnet system (MKD), which deflects the beam horizontally into to a set of Lambertson septum magnets (MSD). The MSD then deflects the beam vertically out of the LHC machine into the MKB dilution kickers which paint the beam onto the graphite dump absorber block (TDE) [1].

Unsynchronised aborts cannot be excluded and could damage downstream accelerator components, in particular the extraction septum magnets, the experimental low-beta triplet magnet apertures and the tertiary collimators. The LBDS includes design features to minimise their frequency [2] and a system of protection devices comprising fixed and moveable diluters and collimators is installed to protect the downstream LHC aperture from the misdirected bunches in case of such a failure. Fig. 1 shows a schematic presentation of the layout and function of the TCDS and TCDQ diluter elements.
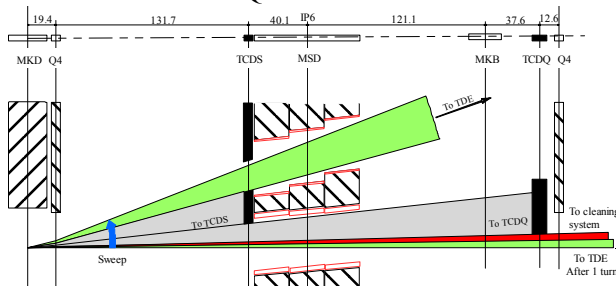

Figure 1: Schematic and functional layout of TCDS and TCDQ diluter elements.

A fixed diluter block (TCDS) [3] is installed immediately upstream of the MSD magnets protecting these from destruction in case the MKD would sweep the beam over the septa. Part of the swept beam could also impact on the Q4 magnets or on other aperture limits in the LHC. In order to protect these elements against damage, a mobile diluter block (TCDQ) [3] and a 2.1 m iron mask (TCDQM) are installed immediately upstream of the Q4 magnets. The TCDQ also protects the LHC arc aperture at 450 GeV, and the low-beta triplet aperture at 7 TeV, from swept bunches and reduces the number of bunches deposited on the collimator jaws.

PERFORMANCE OBJECTIVES

By intercepting 27 proton bunches, at 7 TeV and at ultimate intensity of $2.5 \cdot 10^{11}$ p$^+$/bunch, the TCDQ shall prevent damage to the downstream Q4 superconducting magnets, of which the damage limit is 87 J/cm^3 [4]. Furthermore, at 450 GeV and 7 TeV, the TCDQ intercepts a significant continues beam load from the secondary halo particles and, during a regular beam abort, also any particles which are in the abort gap. These loads shall not exceed the Q4 quench limit of 4 mJ/cm^3 at 7 TeV. During a regular abort, the maximum energy deposition in the superconducting coils should not exceed the quench limit, which is estimated to be $1.4 \cdot 10^{-4}$ of the ultimate beam intensity, or $3 \cdot 10^6$ p$^+$/m.

PROPOSED UPGRADE

Performance Limitations

Currently the TCDQ consists of a 2-tank system per beam, installed on a mobile support girder, with a total length of 6.85 m housing a 6 m long single-sided graphite absorber block (density 1.77 g/cm^3), positioned at ~12.5 m in front of the Q4 magnet. Dynamic stress simulations [5] of possible fault cases and the related damage which could occur to the TCDS have shown that an asynchronous dump of a 7 TeV nominal beam could damage the blocks, the TCDS was modified accordingly [6]. For the same reason, the TCDQ absorber material needs to be changed to a lower density carbon fibre reinforced carbon (CFC), with an increased absorber length, to reduce energy deposition and improve mechanical strength. In addition, simulations [7] have shown that the full LHC beam will penetrate up to 25 m through solid carbon, whereas the range of a single bunch is ~3 m. The installation of a 25 m long absorber would be difficult and only prevents damage in a very specific failure case.

New Composition of the System

A 3-tank system with a total length 10.4 m, with 9 m absorber length will be installed (see Fig. 2). For practical reasons, each tank consists of 12 absorber blocks, made of CFC, having a density of 1.75 or 1.4 g/cm^3.
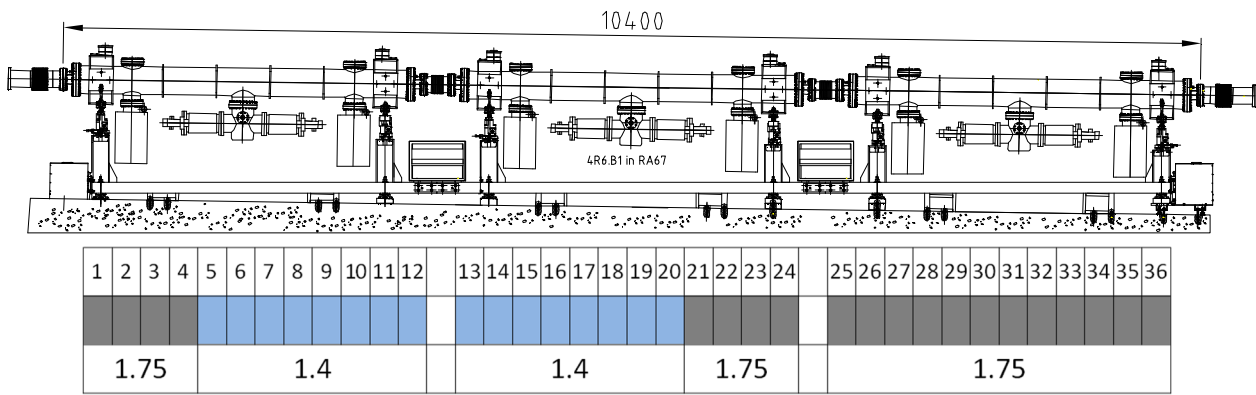
1	2	3	4	5	6	7	8	9	10	11	12		13	14	15	16	17	18	19	20	21	22	23	24		25	26	27	28	29	30	31	32	33	34	35	36
	1.75					1.4										1.4						1.75							1.75							

Figure 2: Proposed layout of a 3-tank TCDQ system (above), with a total length of 10.4 m, installed on a mobile support girder to allow precise positioning of the absorber blocks with respect to the beam position. Below a schematic representation of the 36 absorber blocks inside the tanks with densities of 1.75 or 1.4 g/cm^3.

The manufacture of high density CFC consists of densification the composite by a Chemical Vapour Deposition (CDV) technique which limits the thickness of the blocks to ~40 mm to assure a uniform density. Therefore the presently 75 mm wide absorber blocks will be divided in 2 parts (Fig. 3). Furthermore, since impact of the beam is only in the first ~30 mm of the block, the remainder of the block absorbs the scattered particles, the second part of the block can consist of, cheaper and easier to procure, graphite.
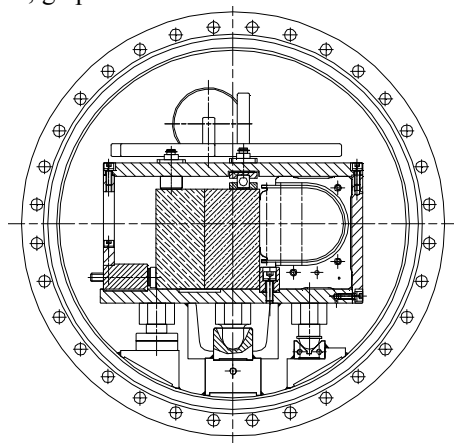

Figure 3: Cross section of the TCDQ structure showing the graphite (left) and CFC (right) absorber blocks.

Improve the Design of VMTAB Bellows

The TCDQ system is connected to the adjacent vacuum chambers by 2 VMTAB bellows, which include impedance shielding and also function as transition from the TCDQ racetrack shaped aperture to the 110 mm circular aperture of the LHC vacuum chambers. To allow the required ±20 mm movement of the TCDQ girder, long RF contact fingers have been used to assure proper shielding. However, due to the stretched length, these fingers have shown to be prone to bulge out during installation or operation. New bellows, with an improved design, will need to be installed to avoid these problems, while at the same time reducing the presently large force needed to offset these bellows.

SIMULATIONS

From FLUKA simulations [8], at nominal intensity, the peak of energy deposited is found to be in the 8th block. The maximum temperature rise is approximately ~454 K while the non-diffusive temperature rise would be ~461 K. At these temperatures the crystal structure is not altered and the dynamical behaviour of the thermally induced elastic waves that will propagate in the structure was investigated. CFC material is modelled as an orthotropic material with the carbon fibre plane being (*0yz*), Fig. 4, with 90º angle between fibre directions.
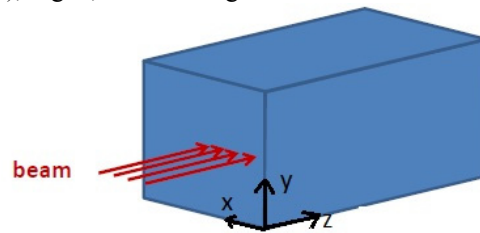

Figure 4: Sketch of the axes, beam and sweep direction.

Numerical simulations of the propagating waves through block 8 are made using AUTODYN® software, while the FLUKA energy deposition [8] is used in the thermo-elasticity equations. The boundary conditions are stress-free such that all waves are reflected back into the material. Initially the thermal shock caused by the beam creates a quick disturbance of primary waves and no shear waves are present before any reflections from the boundaries. After reflection some secondary waves are expected to propagate and AUTODYN® explicit finite element code has the ability to model such phenomena. The Courant–Friedrichs–Lewy (CFL) condition is applied automatically from the smallest element size with an upper bound on the time step. Assuming that the medium is non-dispersive, and since the element size is chosen to be 13 mm such that the smallest wavelengths captured are of the order of the element size, the highest frequency captured is in the order of 10^6 *Hz*. The maximum time step is set such that the cut-off frequency is ~10^8 *Hz* in order that the element size wavelengths are not filtered

out. Material properties are taken from [5] and failure criteria are obtained by comparing simulated stresses to the yield and ultimate allowed stresses in each of the three directions. In case these values are reached, a three dimensional stress failure (Tsai Wu) criterion should have been considered. Highest principal stresses are reached in the *yy* direction and have respective tensile and compressive values of 13.9 MPa and 5.6 Mpa, well below the ~80 MPa yield limits. The maximum tensile stress state happens at the time t = 19.5 μs with the maximum compressive stress state at t = 875 ns, at the end of the energy deposition (Fig. 5).
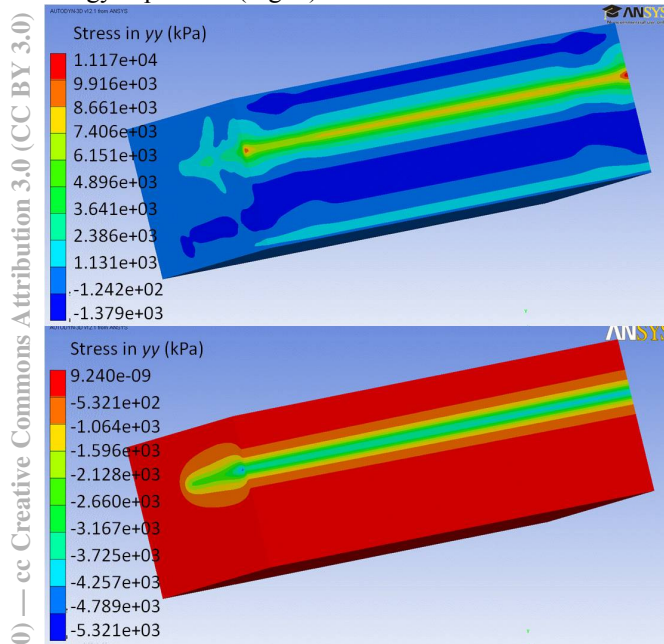

Figure 5: YY stress field (kPa) at t = 19.5 μs (top) and at the end of the energy deposition (bottom).

Fig. 6 shows the order of magnitude of dynamic stresses in *yy* direction vs. time for critical points. Subsequent reflexions from the block boundaries do not yield higher normal stress states and resulting shear stresses do not pose a threat to the structure. Although block 8 has the highest energy deposition which translates into highest peak temperature, block 4 has the highest energy gradient in the (*0y*) direction while block 12 absorbs the highest total energy. Nevertheless, stresses in both of these blocks remain below those of block 8.

As mentioned above, the homogeneous CFC block is cut at x = 40 mm, and the remaining space will be filled with graphite. Since the thermal shock occurring on the graphite part is negligible we are only interested in the reflection/refraction, of the stress wave emerging from the beam location, on the material interface. For simulation, the condition between the two was assumed as bonded, having continuity in all displacements at the material interface. The stress wave propagation direction is mostly (*0y*), parallel to the material interface, yielding similar stresses in the 40 mm CFC part as in the homogeneous material model. Stresses arising in the graphite part are
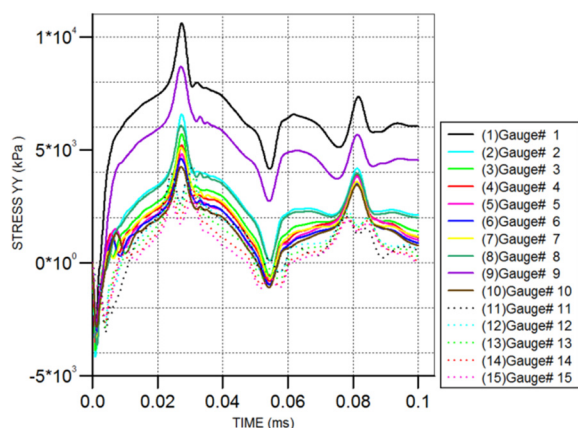

Figure 6: YY stresses vs. time at locations in block 8.

< 3 MPa in compression, which is negligible with respect to the graphite limit of 125 MPa.

A perfectly bounded interface implies that the waves refracted from the CFC part into the graphite part are of maximum amplitude compared to a more realistic condition where the bond is somewhat loose and more reflection back into the CFC part is expected. Simulation of using only the 40 mm CFC part absorbing the load showed similar stresses as for the full block. In reality waves propagating in the (*0x*) direction will tend to be damped out by a greater amount in the full width block, but all simulations assumed a perfectly elastic material with no energy losses which represent the highest possible stress state.

At ultimate LHC beam intensity the maximum temperature rise is ~994 K, still below the temperature limits of the material. Highest compression and tensile stress states reach ~10 MPa at the end of the pulse length, and ~24 MPa after approximately 20 μs respectively, both stress states remain under the material limits

SUMMARY

In order to protect the LHC equipment in the event of an asynchronous beam dump, at ultimate intensity, the currently 6 m long graphite TCDQ absorber needs to be upgraded. Simulations have shown that a 10.4 m long, 3 tank system, with 9 m absorber length containing CFC and graphite blocks with a density of 1.4 and 1.75 g/cm^3 will give sufficient protection.

REFERENCES

[1] O. Brüning et al., ISBN 92-9083-244-0, (2004) Chapter 17.
[2] B. Goddard et al., EPAC'06, Edinburgh, June 2006, TUPLS013, p. 1514 (2006); http://www.JACoW.org
[3] B. Goddard et al., EPAC'04, Lucerne, July 2004, MOPLT038, p. 629 (2004); http://www.JACoW.org
[4] O. Brüning et al., LHC Project Note 141, CERN (1998).
[5] L. Massidda et al., EPAC'06, Edinburgh, June 2006, TUPLS012, p. 1511 (2006); http://www.JACoW.org
[6] W. Weterings, LHCTCDS-ES-0001 rev.2, CERN (2006).
[7] N. A. Tahir, et al., IPAC'11, San Sebastián, September 2011, THPS088, p. 3639 (2011); http://www.JACoW.org
[8] R. Versaci and V. Vlachoudis, ATS-Note-2012-015 MD, CERN (2012).